

Concept of a charged fusion product diagnostic for NSTX

W. U. Boeglin, R. Valenzuela Perez, and D. S. Darrow

Citation: *Rev. Sci. Instrum.* **81**, 10D301 (2010); doi: 10.1063/1.3464262

View online: <http://dx.doi.org/10.1063/1.3464262>

View Table of Contents: <http://rsi.aip.org/resource/1/RSINAK/v81/i10>

Published by the [American Institute of Physics](#).

Related Articles

Boron-rich plasma by high power impulse magnetron sputtering of lanthanum hexaboride
J. Appl. Phys. **112**, 086103 (2012)

Preface: Proceedings of the 19th Topical Conference on High-Temperature Plasma Diagnostics, Monterey, California, USA, 6–10 May 2012
Rev. Sci. Instrum. **83**, 10D101 (2012)

High-resolution charge exchange measurements at ASDEX Upgrade
Rev. Sci. Instrum. **83**, 103501 (2012)

A portable optical emission spectroscopy-cavity ringdown spectroscopy dual-mode plasma spectrometer for measurements of environmentally important trace heavy metals: Initial test with elemental Hg
Rev. Sci. Instrum. **83**, 095109 (2012)

Recent improvements of the JET lithium beam diagnostic
Rev. Sci. Instrum. **83**, 10D533 (2012)

Additional information on Rev. Sci. Instrum.

Journal Homepage: <http://rsi.aip.org>

Journal Information: http://rsi.aip.org/about/about_the_journal

Top downloads: http://rsi.aip.org/features/most_downloaded

Information for Authors: <http://rsi.aip.org/authors>

ADVERTISEMENT



AIP Advances

Now Indexed in Thomson Reuters Databases

Explore AIP's open access journal:

- Rapid publication
- Article-level metrics
- Post-publication rating and commenting

Concept of a charged fusion product diagnostic for NSTX^{a)}

W. U. Boeglin,¹ R. Valenzuela Perez,¹ and D. S. Darrow²¹*Department of Physics, Florida International University, 11200 SW 8th Street, Miami, Florida 33199, USA*²*Princeton Plasma Physics Laboratory, James Forrestal Campus, P.O. Box 451, Princeton, New Jersey 08543, USA*

(Presented 17 May 2010; received 18 May 2010; accepted 2 June 2010; published online 4 October 2010)

The concept of a new diagnostic for NSTX to determine the time dependent charged fusion product emission profile using an array of semiconductor detectors is presented. The expected time resolution of 1–2 ms should make it possible to study the effect of magnetohydrodynamics and other plasma activities (toroidal Alfvén eigenmodes (TAE), neoclassical tearing modes (NTM), edge localized modes (ELM), etc.) on the radial transport of neutral beam ions. First simulation results of deuterium-deuterium (DD) fusion proton yields for different detector arrangements and methods for inverting the simulated data to obtain the emission profile are discussed. © 2010 American Institute of Physics. [doi:10.1063/1.3464262]

I. INTRODUCTION

The products of $d(d,p)t$ and $d(d,{}^3\text{He})n$ reactions, namely, the 3 MeV proton, 1 MeV triton, and 0.8 MeV ${}^3\text{He}$ ion, originate mainly from the neutral beam-plasma interaction and are not confined in NSTX. Due to its relatively small magnetic field ($0.2\text{ T} < B < 0.6\text{ T}$ for the trajectories studied here), the gyroradius of a 3 MeV proton or a 1 MeV triton is between of 0.4 and 1.3 m, which is close to the typical size of the poloidal cross section of the NSTX plasma. Protons and tritons originating in the central region of the plasma can often exit the plasma without completing a full gyro orbit. If one detects these fusion products by selecting a certain particle direction at the location of the detector, one obtains a direct “view” of the DD fusion rate profile in the plasma interior. The data accessible in this manner, which are heavily weighted to the profile of the injection energy beam ions rather than the partially slowed down ions, combined with measurements of the bulk plasma ion density profile, will allow one to determine the neutral beam ion density profile and its variation with time. With typical ion temperatures of $\approx 1\text{ keV}$, the beam-thermal reaction rate is more than a factor of 25 larger than the thermal one. The ratio of beam-beam to beam-thermal reactivity is roughly the ratio of the beam ion density to the thermal ion density, namely 0.13. Consequently, beam-thermal reactions are dominant in NSTX, with beam-beam and thermal reactions suppressed by an order of magnitude. The high time resolution of this system will make it possible to study magnetohydrodynamics (MHD) effects and correlate the proton data with other fast ion loss diagnostics such as scintillator fast lost ion probe,¹ solid-state neutral particle analyzer,² fast-ion D-alpha (FIDA),³ and the neutron detector and provide useful data for energy and momentum transport studies. In addition, the

presence of this diagnostic on NSTX would allow cross comparison with FIDA measurements of the neutral beam ion density profile. This would be of value since the sensitivity of FIDA to beam ions has some pitch angle dependence while the technique proposed here has much less dependence on the pitch angle of the beam ions at their point of sampling. Such a cross comparison of the diagnostics would allow assessment of the degree to which the pitch angle range seen by FIDA drives instabilities or is transported by them.

For this new diagnostic we will use an array of collimated particle detectors arranged in such a way that they measure MeV charged fusion products (CFPs) within well defined bundles of orbits (similar to sight lines) that are crossing the plasma. The detection system, based on solid state detectors and a fast multichannel digitizer, will be able to handle the expected high particle rates (up to a few megahertz) allowing integration times as short as 1 ms, and leading to a time resolution of the same order of magnitude. To explore the potential of this new diagnostic we will build a first version with a total of eight detectors arranged in various configurations.

II. TWO-DIMENSIONAL MODEL

All diagnostics that determined plasma profiles through an inversion technique used quantities which have been integrated along straight lines of sight across the plasma, e.g., x-ray emission and neutron emission. The integration path was therefore very simple and independent of the magnetic field. For the proposed diagnostic however, the integration paths through the plasma are curved and depend on the knowledge of the magnetic field.

Hence, to study the feasibility of an inversion using curved paths we first carried out a two-dimensional (2D) Monte-Carlo simulation of particle production in a simple system consisting of a region with constant magnetic field, a collimator, and a detector. The third dimension was ignored in this case, as in this direction the particles behave like free

^{a)}Contributed paper, published as part of the Proceedings of the 18th Topical Conference on High-Temperature Plasma Diagnostics, Wildwood, New Jersey, May 2010.

ones. The location and the direction of each particle were selected randomly within the constant magnetic field region and given a weight according to the local value of the emissivity. The particle was subsequently counted if its trajectory passed the collimator and hit the detector. The ratio between the number of counted particles and the total number generated corresponds to the total detection efficiency for the detector-collimator configuration ϵ_{2d} . The same quantity can be calculated as follows

$$\epsilon_{2d} = \frac{\int A(\theta) d\theta \int_{\text{orbit}} S(\vec{r}) dl}{2\pi \int \int_{\text{area}} S(\vec{r}) dx dy} \quad (1)$$

Here $A(\theta)$ is the effective detector opening, θ is the incident angle, $S(\vec{r})$ is the emissivity at point \vec{r} , and *orbit* represents the time-reversed particle trajectory. The expression in three dimensions is very similar.⁴ The emissivity $S[\psi(\vec{r})]$ was given as a function of a single variable $\psi(\vec{r})$ which plays the role of poloidal flux of a real system implying constant emissivity on surfaces of constant flux ψ . We introduced some structure into this function to investigate how well it can be reproduced by the inversion procedure using the simulated measurements. In addition this simulation also served as a check of the calculation of the detection efficiency given in Eq. (1). This method has been successfully applied previously in systems detecting CFPs from well defined orbits.⁴⁻⁶ We found that for geometries similar to the one planned for the real system that the two methods agree within the precision of the Monte-Carlo calculation.

To determine S we expressed it as a function of ψ with adjustable parameters. These were then optimized by fitting the integral of the emissivity along the central orbit of the detector-collimator system to the simulated experimental results. The central orbit was defined by the time-reversed proton orbit with its initial position at the center of the collimator and its direction pointing from the center of the detector to the center of the collimator. We used two types of polynomials to represent $S(\psi)$. A “standard” polynomial

$$S(\psi) = a_0 + a_1\psi + a_2\psi^2 + a_3\psi^3 + a_4\psi^4 + a_5\psi^5$$

and a series of Zernike polynomials ${}_n^m Z(r, \theta)$ where for the moment we selected the $m=0$ subset which are radially symmetric polynomials.

$$S(\psi) = a_0 + a_1 \cdot {}_2^0 Z(\psi) + a_2 \cdot {}_4^0 Z(\psi) + a_3 \cdot {}_6^0 Z(\psi) \\ + a_4 \cdot {}_8^0 Z(\psi) + a_5 \cdot {}_{10}^0 Z(\psi).$$

These types of polynomials are being widely used in optics and in x-ray tomographic reconstruction.⁷ To include the fact that experimental data have finite errors we assumed a certain statistical error in the “experimental” data and added corresponding random offsets to each simulated data point according to its precision. These data points together with their errors were subsequently used in the fit procedure described above. The results of one of these fits is shown in Fig. 1. We found that both parameterizations can reproduce the emissivity $S(\psi)$ within each error bar and that the quality of the reconstructed function depends strongly on the precision of the experimental data. The possibility of alpha tomography, which faces a similar problem, has been discussed in Ref. 8.

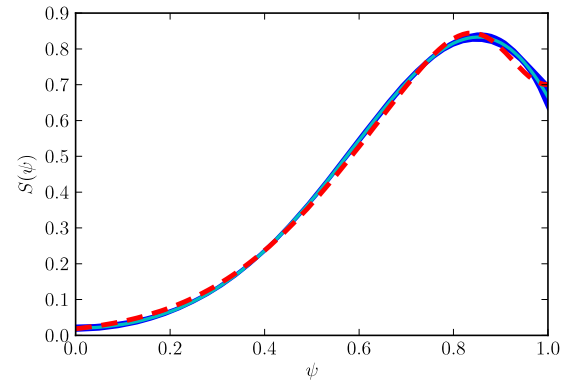


FIG. 1. (Color online) The reconstructed emissivity $S(\psi)$ for the 2D model using a series of Zernike polynomials up to $n=8$ (a total of five parameters) fitted to the simulated data of seven detectors. The dashed line indicates the function used in the simulation and the error band indicates the uncertainty of the fitted function value.

III. SIMULATIONS FOR NSTX

To estimate the proton rates in NSTX we used a LOR-ENTZ orbit code⁵ and placed the detector array at two positions, above and below the midplane. We then calculated the central orbits for the eight detector orientations (Fig. 2). The collimator and the detector active area were selected to be 5×5 mm² and the distance between the collimator and the detector was 50 mm. Assuming a total reaction rate of 2×10^{14} neutrons/s we obtained counts for integration times of 1 and 5 ms. As in the 2D case we added a random deviate to each point according to its error and fitted the pseudodata taking into account their statistical errors. The emissivity was

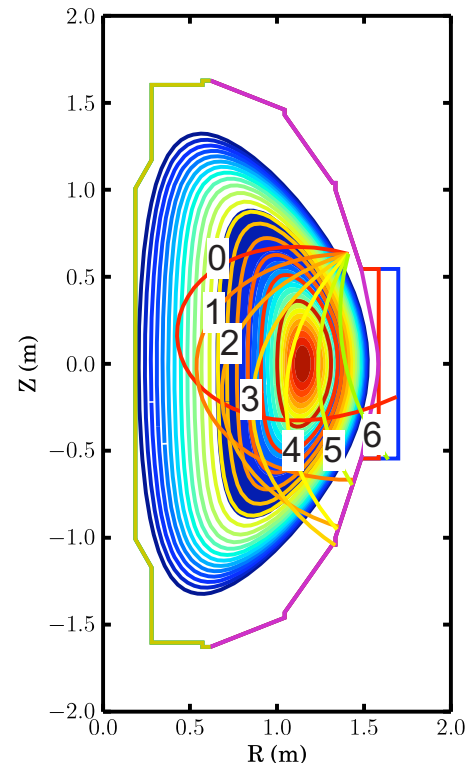


FIG. 2. (Color online) The poloidal view of the NSTX plasma, the limiters, and the detector position above the midplane together with the central orbit associated with each detector in the array. The filled contours represent the emissivity $S(\psi_{\text{rel}})$ and the other ones the relative poloidal flux ψ_{rel} .

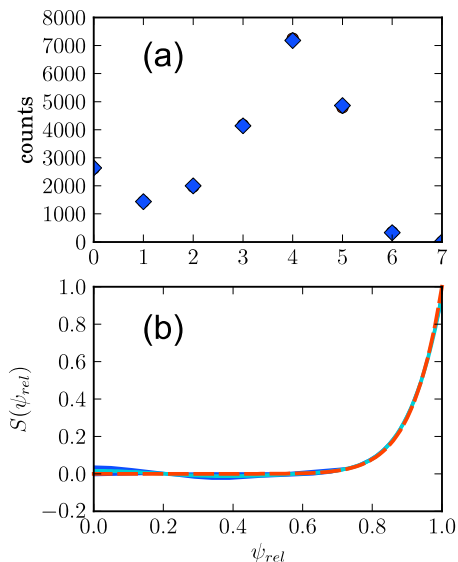


FIG. 3. (Color online) (a) The counts expected for each view shown in Fig. 2 for an integration time of 5 ms together with its fitted value. (b) The fitted emissivity using Zernike polynomials up to $n=10$. The fitted function is represented by the error band and the dashed line indicates the function used for the simulation.

again expressed as a function of ψ_{rel} which is defined in such a way that ψ_{rel} is 1 on the magnetic axis and 0 on the plasma surface. The emissivity used in ORBIT was given by a simple power law $S(\psi_{rel}) = \psi_{rel}^\lambda$ where $\lambda=11.45$ which has described a past experiment but does not necessarily match expectations for the NSTX emission profile.⁹ For both the top as well as the bottom (below the midplane) detector array position the fit was able to reconstruct the emissivity with the top position giving a slightly better reconstruction. The results of the fit for the top position in shown in Fig. 3.

Uniform proton emission on a flux surface is used here as an approximation for the design of a first instrument with a limited number of channels and the interpretation of its data. While beam ion density is not strictly a function of flux surface, the fact that the beams inject tangentially in NSTX means that the beam ions will deviate little more than one gyroradius (about 15 cm) under typical conditions. In case of

changes in the beam ion density profile produced by MHD activity, one might imagine that the underlying plasma equilibrium will not change too drastically, leaving any changes in the signals to be interpreted as real changes in the reactivity along those chords and not just movement of the chords to different parts of the plasma due to changes in the magnetic field. In future studies we plan to include a variation of the emissivity as a function of the poloidal angle θ . This will allow us to investigate the influence of such a variation on the assumption of constant emissivity. We will then test the reconstruction of $S(\psi, \theta)$ using two detector arrays at two different locations with orbits that cross each other.

IV. SUMMARY

The 2D studies as well as the simulations for NSTX with ORBIT have shown that one can obtain the emission profile from an inversion procedure applied to a data set obtained from an array of detectors that are viewing different parts of the plasma cross section. The next step in the development of this diagnostic will be the construction and installation of one or two channels to obtain real data and optimize the final design followed by the construction of the final eight detector system. Depending on the results obtained with the eight channel system, more channels will be considered for a second generation instrument.

ACKNOWLEDGMENTS

This work was supported by the Department of Energy Contract Nos. DESC0001157 and DEAC0209CH11466.

- ¹D. S. Darrow, *Rev. Sci. Instrum.* **79**, 023502 (2008).
- ²D. Liu, W. W. Heidbrink, D. S. Darrow, A. L. Roquemore, S. S. Medley, and K. Shinohara, *Rev. Sci. Instrum.* **77**, 10F113 (2006).
- ³M. Podestá, W. W. Heidbrink, R. E. Bell, and R. Feder, *Rev. Sci. Instrum.* **79**, 10E521 (2008).
- ⁴W. W. Heidbrink and J. D. Strachan, *Rev. Sci. Instrum.* **56**, 501 (1985).
- ⁵J. D. Strachan, *Rev. Sci. Instrum.* **57**, 1771 (1986).
- ⁶R. L. Boivin, C. Kurz, D. H. Lo, C. L. Fiore, R. Granetz, and R. D. Petrasso, *Rev. Sci. Instrum.* **63**, 4533 (1992).
- ⁷R. S. Granetz and P. Smeulders, *Nucl. Fusion* **28**, 457 (1988).
- ⁸N. E. Karulin and S. V. Putvinskij, *Nucl. Fusion* **25**, 961 (1985).
- ⁹J. Felt, C. W. Barnes, R. E. Chrien, S. A. Cohen, W. W. Heidbrink, D. Manos, and S. Zweben, *Rev. Sci. Instrum.* **61**, 3262 (1990).